Effect of Synchronization Errors on the Performance of Multicarrier CDMA Systems

Ying Li and Xiang Gui

Abstract: **A synchronous multicarrier (MC) code-division multiple access (CDMA) system using inverse fast Fourier transform (IFFT) and fast Fourier transform (FFT) for the downlink mobile communication system operating in a frequency selective Rayleigh fading channel is analyzed. Both carrier frequency offset and timing offset are considered in the analysis. Bit error rate performance of the system with both equal gain combining and maximum ratio combining are obtained. The performance is compared to that of the conventional system using correlation receiver. It is shown that when subcarrier number is large, the system using IFFT/FFT has nearly the same performance as the conventional one, while when the subcarrier number is small, the system using IFFT/FFT will suffer slightly worse performance in the presence of carrier frequency offset.**

Index Terms: **Fast Fourier transform (FFT), frequency selective fading, inverse fast Fourier transform (IFFT), multicarrier code-division multiple access (MC-CDMA).**

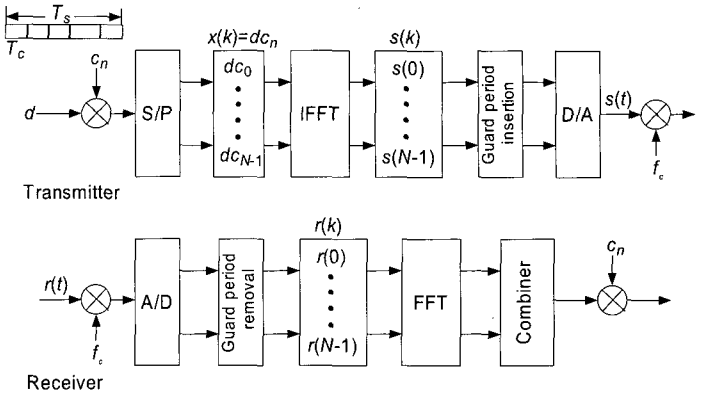

Fig. 1. Block diagram of the MC-CDMA transmitter and receiver using IFFT/FFT.

I. INTRODUCTION

With the increasing demand of high-speed wireless services, future wireless communication system will demand higher data rates. However, when the transmission rate increases, the wireless signal propagation channel tends to suffer from frequency-selective multipath fading. This means that the received signal is composed of several delayed and randomly weighted replicas of the transmitted signal. This gives rise to a form of self-interference, commonly referred to as inter-symbol-interference (ISI). To combat this problem, multi-carrier modulation (MCM) offers an elegant solution.

MCM refers to the generic technique of transmitting high-rate data by dividing it into several parallel lower-rate streams and modulating them concurrently onto separate frequency carriers. By converting a high-rate serial data stream to several parallel low-rate data sub-streams, each sub-stream has longer symbol durations, thus the relative amount of signal dispersion caused by the multipath delay spread is decreased. Multicarrier code-division multiple access (MC-CDMA) [1], [2] is a common form of MCM, which combines orthogonal frequency division multiplexing (OFDM) with the principles of direct sequence code division multiple access (DS-CDMA) [4] with OFDM, and provides a communication system that has the advantages of both.

Due to the advantages of efficient frequency diversity and high bandwidth efficiency, MC-CDMA has received more attention recently. However, a major drawback of multicarrier modulation is its sensitivity to synchronization errors between the transmitter and receiver. Before an MC-CDMA receiver can demodulate the subcarriers, it has to perform at least two synchronization tasks. Firstly, it has to find out where the symbol boundaries are and what the optimal timing instants are to minimize the effects of inter-carrier interference (ICI) and ISI. Secondly, it has to estimate and correct the carrier frequency offsets of the received signal, because frequency offset immediately results in ICI [7]. In an MC-CDMA link, the subcarriers are perfectly orthogonal only if transmitter and receiver use exactly the same frequencies. A related problem is phase noise. A practical oscillator does not produce a carrier at exactly one frequency, but rather a carrier that is phase modulated by random phase jitter. As a result, the frequency, which is the time derivative of the phase, is never perfectly constant, thereby causing ICI in an MC-CDMA receiver. For single carrier systems, phase noise and frequency offsets only give degradation in the received signal to noise ratio (SNR), rather than introducing interference. This is the reason that the sensitivity to phase noise and frequency offset is often mentioned as a major disadvantage of MC-CDMA comparing to single carrier systems.

Recently, there are some papers investigating the effect of frequency offset on MC-CDMA systems. In [8] and [9], the impact of frequency offset on MC-CDMA systems is evaluated for the cases of downlink and uplink Gaussian channels, respectively. The bit error rate (BER) performance of MC-CDMA system with both downlink and uplink frequency selective fading is presented in [10]–[15]. Nevertheless, all of the analyses mentioned above are based on the conventional MC-CDMA system model. A conventional system refers to the one shown in Fig. 1 of [15],

Manuscript received September 7, 2004; approved for publication by Kyungwhoon Cheun, Division II Editor, July 29, 2005.

Y. Li is with the National University of Singapore, Singapore, email: li.ying@nus.edu.sg.

X. Gui is with the Massey University, Singapore, email: X.Gui@massey.ac.nz.

1229-2370/06/$10.00

where a bank of modulators and a bank of demodulators are used at the transmitter and receiver, respectively. For each subcarrier, a modulator/demodulator pair is required. Both modulator and demodulator are analog devices and require a locally generated subcarrier signal in order to perform their tasks. In order to maintain orthogonality among subcarriers, these locally generated subcarriers must have very high precision in frequency, which is difficult to achieve in practice. Furthermore, in MC-CDMA, all subcarriers have identical power. This requires all the modulators and demodulators have equal gain. In practice, it is difficult to adjust the gain of an analog device to a precise value. Making the gains of two analog devices to be exactly the same is impossible. Notice that the demodulator used in conventional system is essentially a correlator, which consists of a multiplier and an integrator. It is an optimum demodulator when rectangular symbol pulse is employed in the presence of white Gaussian noise. Therefore, conventional system model is often adopted in theoretical analysis of MC-CDMA performance [1], [8], [10]–[15]. However, it is obvious that direct implementation of the conventional system is not feasible.

Fortunately, it has been found that multicarrier modulation and demodulation can be easily implemented by IFFT and FFT, respectively [2], [5]. As shown in Fig. 1, the IFFT/FFT-based approach employs IFFT and FFT instead of the bank of modulators and the bank of demodulators, thus converting analog process to digital processing at both the transmitter and the receiver. The IFFT/FFT-based MC-CDMA is equivalent to the conventional one under ideal conditions, i.e., constant channel characteristics over the symbol duration, ideal carrier frequency synchronization, and ideal symbol timing synchronization. However, in real life situations synchronization errors always exist. It is therefore interesting to investigate whether the two systems still perform identically in the presence of carrier frequency offset and symbol timing offset. This topic is important since it helps to establish a link between theoretical study based on conventional system model and practical implementation based on FFT processing. The rest of this paper presents a detailed study on the topic. Moreover, although many research works have been done to analyze the effect of carrier frequency offset, the effect of timing offset seems to be neglected, and the analyses of system performance with both frequency offset and timing offset are absent in the open literatures. These topics will also be discussed in our paper.

The rest of this paper is organized as follows: The downlink MC-CDMA system model using IFFT/FFT is described in Section II. The channel model is presented in Section III. The BER performance is analyzed in Section IV. Section V provides numerical results and discussions, while Section VI concludes the paper.

II. DOWNLINK MC-CDMA SYSTEM MODEL

The transmitter and receiver of the MC-CDMA system using IFFT/FFT are shown in Fig. 1. At the transmitter, the data symbol with duration T_s is first spread by a pseudo-noise (PN) sequence with period N and *chip duration* T_c, and then converted into parallel streams, which are transmitted over multiple subcarriers. For clarity of analysis, we assume that the spreading factor of the system is equal to the number of subcarriers N, for BPSK modulation, the new chip duration on each parallel stream is equal to the *symbol duration*, that is T_s. Notice that multiple data bits can be easily accommodated in one symbol duration by increasing the number of subcarriers and the analysis presented in this paper can be readily extended to such cases. 4 Successive subcarriers are separated by $\Delta f = 1/T_s$ Hz. Thus the frequency spectrums of successive carriers overlap. Since the symbol duration is much larger than the chip duration, the amount of time dispersion caused by multipath delay spread is only a small portion of the symbol duration and the effect of ISI is decreased. Different users transmit at the same set of subcarriers but with a different spreading code. To further alleviate the effect of ISI, a guard period T_G is inserted at the beginning of each symbol. The guard period is the copy of the last T_G portion of the symbol. As shown in Fig. 1, the modulation and demodulation processes can be implemented by efficient IFFT and FFT, respectively.

Suppose there are M simultaneous active users, user m transmits data bit d_m with a spreading code $\{c_{n,m}, n = 0, 1, \cdots, N-1\}$ over the zero-th symbol duration $[0, NT_c]$, according to the block diagram shown in Fig. 1, the output of the IFFT block can be represented by

$$s_k = \sum_{m=0}^{M-1} \sum_{n=0}^{N-1} d_m c_{n,m} e^{j2\pi nk/N}, \qquad k = 0, 1, \cdots, N-1 \quad (1)$$

where N is the number of subcarriers and M is the number of users. Assuming that the digital to analog converter (DAC) is ideal and does not introduce any distortion, the transmitted lowpass equivalent downlink MC-CDMA signal of the zero-th symbol can be written as

$$s(t) = \sum_{m=0}^{M-1} \sum_{n=0}^{N-1} d_m c_{n,m} e^{j2\pi \frac{n}{NT_c} t}, \qquad 0 \le t \le NT_c \quad (2)$$

where $\frac{n}{NT_c}$ is the lowpass frequency of the n-th subcarrier. Comparing (1) and (2), it can be seen that $s_k = s(kT_c)$.[1] Note that the guard period of the zero-th symbol is inserted over the duration $[-T_G, 0)$ and is the copy of $s(t)$ over $[NT_c - T_G, NT_c)$. Since all the subcarriers have integer number of cycles over the duration NT_c, the zero-th symbol waveform can be represented by $s(t)$ defined over $[-T_G, NT_c]$.

III. CHANNEL MODEL

We consider a frequency selective multipath slow Rayleigh fading channel where the fading characteristic is constant over at least one symbol duration. In open literatures the frequency selective multipath Rayleigh fading channel is commonly modeled by the finite length tapped delay line [17], [18] as shown in Fig. 2. Using the n-th subcarrier as the input to the tapped delay line and observing the corresponding output, it is easy to

[1] In this paper, the size of IFFT is assumed to be N. This assumption is employed only for clear presentation of the concept. According to the sampling theorem, at least $2N$ samples are required to construct the analog waveform of one MC-CDMA symbol. Hence in implementation, the size of IFFT should be at least $2N$.

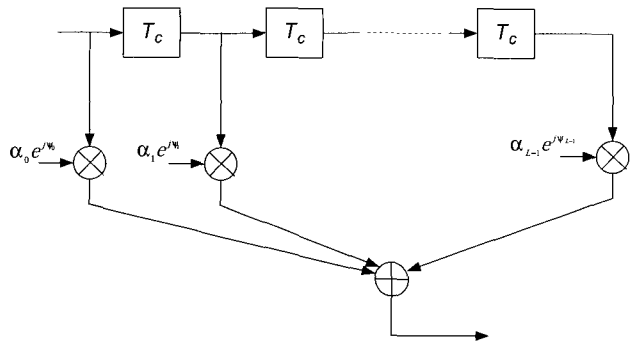

Fig. 2. Multipath channel model (complex baseband representation).

show that the equivalent complex channel gain h_n for the n-th subcarrier can be represented by the complex multipath gains in the following equation

$$h_n = \sum_{l=0}^{L-1} \alpha_l e^{j\psi_l} e^{-j\omega_n(lT_c)} \tag{3}$$

where L is the number of multipaths, $\{\alpha_l, l = 0, 1, \cdots, L-1\}$ are the multipath envelopes which are independent Rayleigh random variables (r.v.'s), $\{\psi_l, l = 0, 1, \cdots, L-1\}$ are the multipath phases which are independent, identically distributed (i.i.d.) r.v.'s uniform in $(0, 2\pi)$, and ω_n is the angular frequency of the n-th subcarrier. Notice that $\{\psi_l\}$ is independent of $\{\alpha_l\}$. Equation (3) can be further rewritten as

$$h_n = \beta_n e^{j\Phi_n} \tag{4}$$

where β_n and Φ_n are the magnitude and phase of the channel gain for the n-th subcarrier, respectively. As can be seen from (3) and (4), although the channel is frequency selective, the narrowband signal transmitted over each subcarrier experiences frequency nonselective Rayleigh fading. Channel gains for subcarriers are identically distributed zeromean complex Gaussian r.v.'s and are mutually correlated. The variance of h_n is denoted as σ^2. The maximum delay due to multipath is $(L-1)T_c$, which is referred to as channel delay spread T_d. Defining Ω_l as the second moment of $\{\alpha_l\}$ (i.e., $\Omega_l = E[(\alpha_l)^2]$), we assume

$$\Omega_l = \Omega_0 e^{-\delta l}, \qquad \delta \geq 0. \tag{5}$$

Equation (5) accounts for the decay of average path strength as a function of path delay. The parameter δ reflects the rate at which this decay occurs. The shape of the decay function is referred to as the multipath intensity profile (MIP) [19]. Exponential MIP is assumed in this paper. Actual measurements indicate that this is fairly accurate for a congested urban area [19].

IV. PERFORMANCE ANALYSIS

After passing though the multipath channel, the received ISI-free part of the zero-th symbol takes the form

$$r(t) = \sum_{m=0}^{M-1}\sum_{n=0}^{N-1} d_m c_{n,m} \beta_n e^{j\Phi_n} e^{j2\pi(\frac{n}{NT_c}+\delta f)t} + \eta(t), \quad -(T_G - T_d) \leq t \leq NT_c \tag{6}$$

where $\eta(t)$ is the lowpass equivalent of the additive white Gaussian noise (AWGN) with zero mean and unilateral power spectral density N_0 and δf is the frequency offset. After sampling, the signal sample at $t = kT_c + \tau$ is given by

$$r(kT_c+\tau) = \sum_{m=0}^{M-1}\sum_{n=0}^{N-1} d_m c_{n,m} \beta_n e^{j\Phi_n} e^{j2\pi(\frac{n}{NT_c}+\delta f)(kT_c+\tau)} + \eta(kT_c+\tau) \tag{7}$$

where τ is the timing offset. To avoid the complicated case of ISI, we assume $-(T_G - T_d) \leq \tau \leq 0$. It is well known that the practical design choice is to make the symbol duration at least five times the guard time [3]. Here we chose guard period to be 20% of T_s, to make the guard time loss smaller than 1 dB. Hence the timing offset value should be kept below this value.

Assuming that user p is the reference user and the frequency offset is less than Δf, as shown in Appendix A, the p-th user's i-th chip obtained after FFT operation is found to be

$$\begin{aligned}\hat{d}_{i,p} &= \frac{1}{N}\sum_{k=0}^{N-1} r(kT_c+\tau) e^{-j2\pi ki/N} \\ &= \frac{1}{N} P \cdot e^{j\frac{2\pi}{N}\cdot\frac{\tau}{T_c}(i+\frac{\delta f}{\Delta f})} d_p c_{i,p} \beta_i e^{j\Phi_i} \\ &+ \frac{1}{N}\sum_{\substack{m=0\\ m\neq p}}^{M-1} P \cdot e^{j\frac{2\pi}{N}\cdot\frac{\tau}{T_c}(i+\frac{\delta f}{\Delta f})} d_p c_{i,m} \beta_i e^{j\Phi_i} \\ &+ \frac{1}{N}\sum_{m=0}^{M-1}\sum_{\substack{n=0\\ n\neq i}}^{N-1} Q(n,i) \cdot e^{j\frac{2\pi}{N}\cdot\frac{\tau}{T_c}(n+\frac{\delta f}{\Delta f})} d_m c_{n,m} \beta_n e^{j\Phi_n} \\ &+ \eta_i'\end{aligned} \tag{8}$$

where

$$P = \frac{e^{j2\pi\frac{\delta f}{\Delta f}} - 1}{e^{j2\pi\frac{\delta f}{N\cdot\Delta f}} - 1},$$

$$Q(n,i) = \frac{e^{j2\pi(n-i+\frac{\delta f}{\Delta f})} - 1}{e^{j2\pi(n-i+\frac{\delta f}{\Delta f})/N} - 1}.$$

It is easy to show that after FFT, the resultant noise component η_i', is still Gaussian.

Normally, there are two ways of combining the chips of the same data bit: Equal gain combining (EGC) and maximum ratio combining (MRC). Both will be studied in the following.

A. Equal Gain Combining

With EGC, knowledge of $\{\Phi_i, i = 0, 1, \cdots, N-1\}$ is assumed known at the receiver. After despreading with EGC, the signal obtained can be written as

$$\hat{d}_p = \sum_{i=0}^{N-1} \hat{d}_{i,p} \cdot c_{i,p} e^{-j\Phi_i} = \sum_{i=0}^{N-1} \hat{d}'_{i,p} \tag{9}$$

where

$$\hat{d}'_{i,p} = \eta'_i c_{i,p} e^{-j\Phi_i} + \frac{1}{N} P \cdot e^{j\frac{2\pi}{N}\cdot\frac{\tau}{T_c}(i+\frac{\delta f}{\Delta f})} d_p \beta_i + \sum_{\substack{m=0 \\ m\neq p}}^{M-1} P \cdot e^{j\frac{2\pi}{N}\cdot\frac{\tau}{T_c}(i+\frac{\delta f}{\Delta f})} d_m c_{i,m} c_{i,p} \beta_i + \sum_{m=0}^{M-1} \sum_{\substack{n=0 \\ n\neq i}}^{N-1} \frac{Q(n,i)}{N} e^{j\frac{2\pi}{N}\frac{\tau}{T_c}(n+\frac{\delta f}{\Delta f})} d_m c_{n,m} c_{i,p} \beta_n \times e^{j(\Phi_n - \Phi_i)}. \quad (10)$$

Thus, (9) can be rewritten as

$$\hat{d}_p = \sum_{i=0}^{N-1} d'_{i,p} = \sum_{i=0}^{N-1} \eta'_i \cdot c_{i,p} e^{-j\Phi_i} + \frac{P}{N} \sum_{i=0}^{N-1} e^{j\frac{2\pi}{N}\cdot\frac{\tau}{T_c}(i+\frac{\delta f}{\Delta f})} d_{i,p} \beta_i + \frac{P}{N} \sum_{i=0}^{N-1} \sum_{\substack{m=0 \\ m\neq p}}^{M-1} e^{j\frac{2\pi}{N}\cdot\frac{\tau}{T_c}(i+\frac{\delta f}{\Delta f})} d_{i,m} c_{i,m} c_{i,p} \beta_i + \sum_{i=0}^{N-1} \sum_{m=0}^{M-1} \sum_{\substack{n=0 \\ n\neq i}}^{N-1} \frac{Q(n,i)}{N} e^{j\frac{2\pi}{N}\frac{\tau}{T_c}(i+\frac{\delta f}{\Delta f})} d_{n,m} c_{n,m} c_{i,p} \beta_n \times e^{j(\Phi_n - \Phi_i)}. \quad (11)$$

The decision variable U_p is obtained by taking the real part of $\hat{d}_p$ (See Appendix B)

$$U_p = \sum_{i=0}^{N-1} P' \cdot d_{i,p} \beta_i + \sum_{i=0}^{N-1} \sum_{\substack{m=0 \\ m\neq p}}^{M-1} P' \cdot d_{i,m} c_{i,m} c_{i,p} \beta_i + \sum_{i=0}^{N-1} \sum_{m=0}^{M-1} \sum_{\substack{n=0 \\ n\neq i}}^{N-1} Q'(n,i) \cdot d_m c_{n,m} c_{i,p} \beta_n + \mathrm{Re}\Big(\sum_{i=0}^{N-1} \eta'_i \cdot c_{i,p} e^{-j\Phi_i}\Big) \quad (12)$$

where

$$P' = \frac{\cos[(1-\frac{1}{N})\cdot\pi\cdot\frac{\delta f}{\Delta f} + \frac{2\pi}{N}\cdot\frac{\tau}{T_c}(i+\frac{\delta f}{\Delta f})]\sin(\pi\frac{\delta f}{\Delta f})}{N\cdot\sin(\pi\frac{\delta f}{N\cdot\Delta f})}. \quad (13)$$

The decision variable U_p can be divided into five parts

$$U_p = D_p + \xi + ICI_1 + ICI_2 + MAI. \quad (15)$$

The term D_p is the desired output

$$D_p = \sum_{i=0}^{N-1} P' \cdot d_{i,p} \beta_i. \quad (16)$$

The term $\xi = \mathrm{Re}(\sum_{i=0}^{N-1} \eta'_i \cdot c_{i,p} e^{-j\Phi_i})$ is the interference term due to Gaussian noise. It is easy to see that ξ is Gaussian with zero mean and variance $N_0 N$. The two terms of ICI: ICI_1 is the interference from same user, due to different subcarriers

$$ICI_1 = \sum_{i=0}^{N-1} \sum_{\substack{n=0 \\ n\neq i}}^{N-1} Q'(n,i) \cdot d_{n,p} c_{n,p} c_{i,p} \beta_n \quad (17)$$

while ICI_2 is the interference from other users, due to different subcarriers

$$ICI_2 = \sum_{i=0}^{N-1} \sum_{\substack{m=0 \\ m\neq p}}^{M-1} \sum_{\substack{n=0 \\ n\neq i}}^{N-1} Q'(n,i) \cdot d_{n,m} c_{n,m} c_{i,p} \beta_n. \quad (18)$$

MAI is the interference from other users, due to same subcarriers

$$MAI = \sum_{i=0}^{N-1} \sum_{\substack{m=0 \\ m\neq p}}^{M-1} P' \cdot d_{i,m} c_{i,m} c_{i,p} \beta_i. \quad (19)$$

It is easy to see that the mean and variance of the signal will depend on the correlation conditions of the subcarrier channel gains. Following our channel model, all the subcarrier channel gains are mutually correlated. However, many previous researches employed the common assumption of independent subcarrier channel gains [10], [11], [13]. In order to compare the results of this paper with previous research under the same conditions, we consider two cases in the sequel.

A.1 *Case 1:* $\{h_n, n = 0, 1, \cdots, N-1\}$ *are Mutually Independent*

As shown in Appendix C, the interference terms ICI_1, ICI_2, and MAI are Gaussian with zero mean and variances

$$Var[ICI_1] = \sum_{i=0}^{N-1} \sum_{\substack{n=0 \\ n\neq i}}^{N-1} Var[Q'(n,i)\beta_n] \quad (20)$$

$$Var[ICI_2] = (M-1)\cdot \sum_{i=0}^{N-1} \sum_{\substack{n=0, \\ n\neq i}}^{N-1} Var[Q'(n,i)\beta_n] \quad (21)$$

$$Var[MAI] = (M-1)\cdot P'^2 \cdot \sum_{i=0}^{N-1} Var[\beta_i]. \quad (22)$$

Assuming a "one" is transmitted, then the mean and variance of U_p are given, respectively, by

$$E(U_p) = P' \cdot \sum_{i=0}^{N-1} E(\beta_i) \quad (23)$$

$$Q'(n,i) = \frac{\cos[\pi(n-i+\frac{\delta f}{\Delta f})(1-\frac{1}{N}) + \frac{2\pi}{N}\cdot\frac{\tau}{T_c}(i+\frac{\delta f}{\Delta f}) + (\Phi_n - \Phi_i)]\sin[\pi(n-i+\frac{\delta f}{\Delta f})]}{N\cdot\sin[\pi(n-i+\frac{\delta f}{\Delta f})/N]} \quad (14)$$

and

$$Var(U_p) = P'^2 \sum_{i=0}^{N-1} Var(\beta_i) + N_0 N + \sum_{i=0}^{N-1} \sum_{\substack{n=0 \\ n\neq i}}^{N-1} Var[Q'(n,i)\beta_n] + (M-1) \sum_{i=0}^{N-1} \sum_{\substack{n=0, \\ n\neq i}}^{N-1} Var[Q'(n,i)\beta_n] + (M-1)P'^2 \sum_{i=0}^{N-1} Var[\beta_i]. \quad (24)$$

The probability of error or average BER is given by

$$P(e) = \frac{1}{2} erfc\left(\frac{E(U_p)}{\sqrt{2Var(U_p)}}\right). \quad (25)$$

A.2 *Case 2:* $\{h_n, n = 0, 1, \cdots, N-1\}$ *are Mutually Correlated*

In this case, U_p is conditional Gaussian conditioned on $\{\beta_n\}$ and $\{\Phi_n\}$. As shown in Appendix C, the conditional variances of ICI_1, ICI_2, and MAI can be obtained as, respectively

$$Var[ICI_1|\{\beta_n\},\{\Phi_n\}] = \sum_{i=0}^{N-1} \sum_{\substack{n=0 \\ n\neq i}}^{N-1} [Q'(n,i)]^2 \beta_n^2 \quad (26)$$

$$Var[ICI_2|\{\beta_n\},\{\Phi_n\}] = (M-1) \cdot \sum_{i=0}^{N-1} \sum_{\substack{n=0, \\ n\neq i}}^{N-1} [Q'(n,i)]^2 \beta_n^2 \quad (27)$$

$$Var[MAI|\{\beta_n\},\{\Phi_n\}] = (M-1) \cdot P'^2 \cdot \sum_{i=0}^{N-1} \beta_i^2. \quad (28)$$

Hence, the mean and variance of U_p conditioned on $\{\beta_n\}$ and $\{\Phi_n\}$ are changed to

$$E(U_p|\{\beta_n\},\{\Phi_n\}) = P' \cdot \sum_{i=0}^{N-1} \beta_i \quad (29)$$

and

$$Var(U_p|\{\beta_n\},\{\Phi_n\}) = N_0 N + \sum_{i=0}^{N-1} \sum_{\substack{n=0 \\ n\neq i}}^{N-1} [Q'(n,i)]^2 \beta_n^2 + (M-1) \cdot \sum_{i=0}^{N-1} \sum_{\substack{n=0, \\ n\neq i}}^{N-1} [Q'(n,i)]^2 \beta_n^2 + (M-1) \cdot P'^2 \cdot \sum_{i=0}^{N-1} \beta_i^2 \quad (30)$$

respectively. The probability of error conditioned on $\{\beta_n\}$ and $\{\Phi_n\}$ is simply given by

$$P[e|\{\beta_n\},\{\Phi_n\}] = \frac{1}{2} erfc\left(\frac{E(U_p|\{\beta_n\},\{\Phi_n\})}{\sqrt{2Var(U_p|\{\beta_n\},\{\Phi_n\})}}\right) \quad (31)$$

and the BER is obtained by averaging (31) over $\{\beta_0, \beta_1, \cdots, \beta_{N-1}\}$ and $\{\Phi_0, \Phi_1, \cdots, \Phi_{N-1}\}$.

The average SNR is defined by

$$SNR = \frac{T_s}{2N_0 N} E[(\sum_{n=0}^{N-1} \beta_n)^2]. \quad (32)$$

The evaluation of (31) and (32) can be done by Monte Carlo integration [20].

B. Maximum Ratio Combining

For MRC, the complex channel gain of each subcarrier must be continuously estimated, which may not be feasible in practice. However, MRC gives a lower bound of the system BER. With MRC, (9) can be rewritten as

$$\begin{aligned} \hat{d}_p &= \sum_{i=0}^{N-1} \hat{d}_{i,p} c_{i,p} \beta_i e^{-j\Phi_i} \\ &= \sum_{i=0}^{N-1} \eta_i' \cdot c_{i,p} \beta_i e^{-j\Phi_i} + \sum_{i=0}^{N-1} P' e^{j\frac{2\pi}{N} \cdot \frac{\tau}{T_c}(i+\frac{\delta f}{\Delta f})} d_{i,p} \beta_i^2 \\ &+ \sum_{i=0}^{N-1} \sum_{\substack{m=0 \\ m\neq p}}^{M-1} P' e^{j\frac{2\pi}{N} \cdot \frac{\tau}{T_c}(i+\frac{\delta f}{\Delta f})} d_{i,m} c_{i,m} c_{i,p} \beta_i^2 \\ &+ \sum_{i=0}^{N-1} \sum_{m=0}^{M-1} \sum_{\substack{n=0 \\ n\neq i}}^{N-1} Q'(n,i) \cdot e^{j\frac{2\pi}{N} \cdot \frac{\tau}{T_c}(i+\frac{\delta f}{\Delta f})} d_{n,m} c_{n,m} c_{i,p} \beta_n \beta_i \end{aligned} \quad (33)$$

and (16)–(19) become

$$D_p = \sum_{i=0}^{N-1} P' \cdot d_{i,p} \beta_i^2 \quad (34)$$

$$ICI_1 = \sum_{i=0}^{N-1} \sum_{\substack{n=0 \\ n\neq i}}^{N-1} Q'(n,i) \cdot d_{n,p} c_{n,p} c_{i,p} \beta_i \beta_n \quad (35)$$

$$ICI_2 = \sum_{i=0}^{N-1} \sum_{\substack{m=0 \\ m\neq p}}^{M-1} \sum_{\substack{n=0 \\ n\neq i}}^{N-1} Q'(n,i) \cdot d_{n,m} c_{n,m} c_{i,p} \beta_i \beta_n \quad (36)$$

and

$$MAI = \sum_{i=0}^{N-1} \sum_{\substack{m=0 \\ m\neq p}}^{M-1} P' \cdot d_{i,m} c_{i,m} c_{i,p} \beta_i^2 \quad (37)$$

respectively. Hence for case 1, the variances given in (26)–(28) are changed to

$$Var[ICI_1] = \sum_{i=0}^{N-1} \sum_{\substack{n=0 \\ n\neq i}}^{N-1} Var[Q'(n,i) \cdot \beta_n \beta_i] \quad (38)$$

$$Var[ICI_2] = (M-1) \cdot \sum_{i=0}^{N-1} \sum_{\substack{n=0, \\ n\neq i}}^{N-1} Var[Q'(n,i) \cdot \beta_n \beta_i] \quad (39)$$

$$Var[MAI] = (M-1) \cdot P'^2 \cdot \sum_{i=0}^{N-1} Var(\beta_i^2) \quad (40)$$

respectively.

Using (25), we can obtain the system BER with MRC, with $E(U_p)$ equals $E(D_p)$ obtained from (34), $Var(U_p)$ equals the sum of $Var[ICI_1]$, $Var[ICI_2]$, and $Var[MAI]$ given by (38)–(40) and the variances of D_p and ξ.

For case 2, the system BER with MRC can also be evaluated by following a similar procedure as that described for EGC.

C. Discussion

Observing (8), the attenuation factor P/N can be represented as

$$\begin{aligned}\frac{1}{N}P &= \frac{1}{N}\frac{e^{j2\pi\frac{\delta f}{\Delta f}}-1}{e^{j2\pi\frac{\delta f}{N\cdot\Delta f}}-1} \\ &= \frac{1}{N}\frac{\cos\left(2\pi\frac{\delta f}{\Delta f}\right)+j\sin\left(2\pi\frac{\delta f}{\Delta f}\right)-1}{\cos\left(2\pi\frac{\delta f}{N\cdot\Delta f}\right)+j\sin\left(2\pi\frac{\delta f}{N\cdot\Delta f}\right)-1}\end{aligned} \tag{41}$$

thus, when $N >> 1$ and $\frac{\delta f}{\Delta f} < 1$, $\cos\left(2\pi\frac{\delta f}{N\cdot\Delta f}\right) \cong 1$ and $\sin\left(2\pi\frac{\delta f}{N\cdot\Delta f}\right) \cong 2\pi\frac{\delta f}{N\cdot\Delta f}$, (41) is approximated by

$$\frac{\left(\cos\left(2\pi\frac{\delta f}{\Delta f}\right)-1\right)+j\sin\left(2\pi\frac{\delta f}{\Delta f}\right)}{j2\pi\frac{\delta f}{\Delta f}}. \tag{42}$$

The numerator of (42) is complex valued. Its amplitude can be found as follows

$$\begin{aligned}&\sqrt{\left(\cos\left(2\pi\frac{\delta f}{\Delta f}\right)-1\right)^2+\sin^2\left(2\pi\frac{\delta f}{\Delta f}\right)} \\ &= \sqrt{2\left(1-\cos\left(2\pi\frac{\delta f}{\Delta f}\right)\right)} \\ &= \sqrt{2\cdot 2\sin^2\left(\pi\frac{\delta f}{\Delta f}\right)} = 2\sin\left(\pi\frac{\delta f}{\Delta f}\right)\end{aligned} \tag{43}$$

and its phase can be determined as

$$\begin{aligned}&\mathrm{tg}^{-1}\frac{\sin\left(2\pi\frac{\delta f}{\Delta f}\right)}{\left(\cos\left(2\pi\frac{\delta f}{\Delta f}\right)-1\right)} = \mathrm{tg}^{-1}\frac{2\sin\left(\pi\frac{\delta f}{\Delta f}\right)\cos\left(\pi\frac{\delta f}{\Delta f}\right)}{-2\sin^2\left(\pi\frac{\delta f}{\Delta f}\right)} \\ &= \mathrm{tg}^{-1}\left(\frac{\cos\left(\pi\frac{\delta f}{\Delta f}\right)}{-\sin\left(\pi\frac{\delta f}{\Delta f}\right)}\right) = \pi\frac{\delta f}{\Delta f}+\frac{\pi}{2}\end{aligned} \tag{44}$$

Therefore, (42) can be rewritten as

$$\frac{\sin\left(\pi\frac{\delta f}{\Delta f}\right)}{\pi\frac{\delta f}{\Delta f}}e^{j\pi\frac{\delta f}{\Delta f}}. \tag{45}$$

Taking the real part of (45), we have

$$\frac{\sin\left(\pi\frac{\delta f}{\Delta f}\right)}{\pi\frac{\delta f}{\Delta f}}\cos\left(\pi\frac{\delta f}{\Delta f}\right). \tag{46}$$

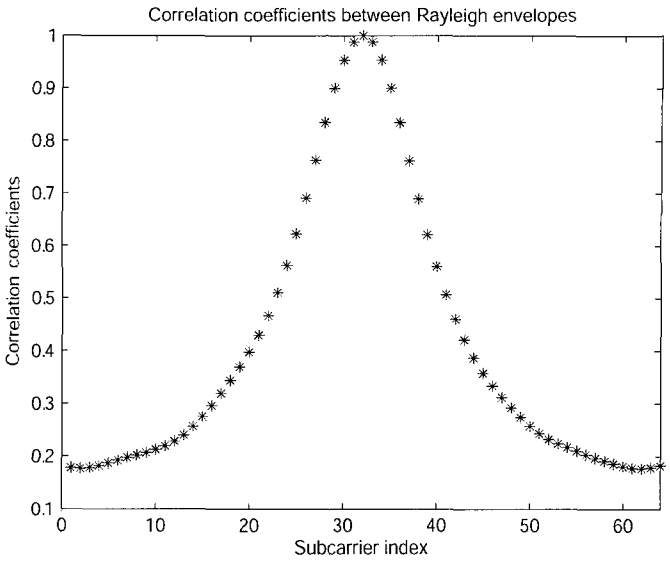

Fig. 3. Correlation coefficients between β_n and β_{31}.

Compared to the analytical result in [13], we can see that (46) is identical to the factor $\frac{\sin(\pi\Delta)}{\pi\Delta}\cos(\pi\Delta)$ as in [13], taking into consideration that different notations are used. Equation (46) can also be readily obtained if we apply the same approximation to P'. Although only the zero-th symbol is considered in the above comparison, it is natural to infer that similar equivalence exists for other symbols. Therefore, we can conclude that in the presence of frequency offset, for $N >> 1$, the performance of FFT-based system is almost identical to that of conventional system. However, for small values of N, e.g., $N = 16$, it can be shown that the difference between amplitudes of (8) and (9) is in the order of 10^{-3} when $\frac{\delta f}{\Delta f} \geq 0.489$. This may lead to noticeable difference in BER performance.

V. NUMERICAL RESULT

The effect of frequency offset on BER performance is studied by numerical evaluation of (31). We set $N = 64$ and $L = 6$. We assume that the power of each multipath is 4 dB less than that of its neighboring early path, thus δ is approximately $0.9210(-\log(1 \times 10^{-0.4}))$. We use the following method to generate correlated subcarrier channel gains $\{\beta_n e^{j\Phi_n}\}$: First, we generate a set of i.i.d. complex Gaussian r.v.'s. Then, we set the power of these r.v.'s according to the exponential MIP to generate L complex multipath gains $\alpha_i e^{j\psi_i}, i = 0, 1, \cdots, L-1$. Finally, we obtain the complex channel gain for the n-th subcarrier by using (3). Thus, the Rayleigh envelopes $\{\beta_n\}$ generated are correlated, and so are the phases $\{\Phi_n\}$. A total of 5000 realizations of $\{\beta_n e^{j\Phi_n}\}$ are generated. The correlation coefficients between Rayleigh envelops $\{\beta_n, n = 0, 1, \cdots, 63\}$ and β_{31} used in the evaluation are shown in Fig. 3.

Fig. 4 shows the BER curves of the MC-CDMA system with 64 subcarriers and 10 users experiencing various carrier frequency offsets and timing offsets. EGC is used at the receiver. As the degree of offsets increases, so does the performance deterioration. Because both the frequency offset and the timing

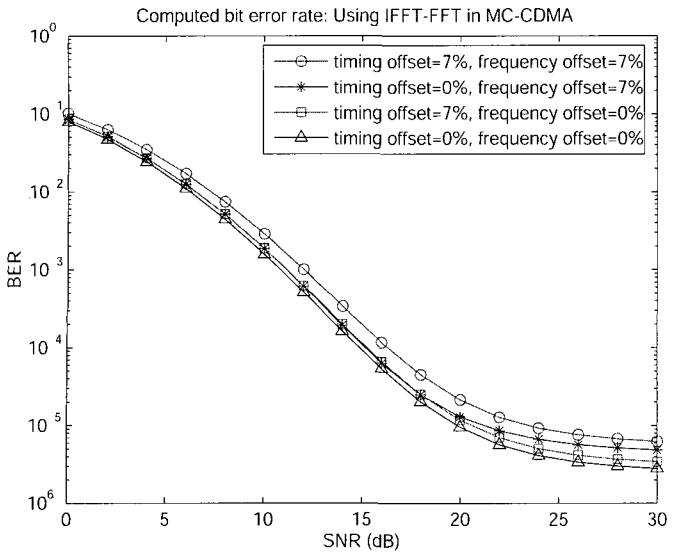

Fig. 4. BERs of an MC-CDMA system with 64 subcarriers and 10 users experiencing carrier frequency offset and timing offset in percentage of Δf and T_s, respectively. (EGC)

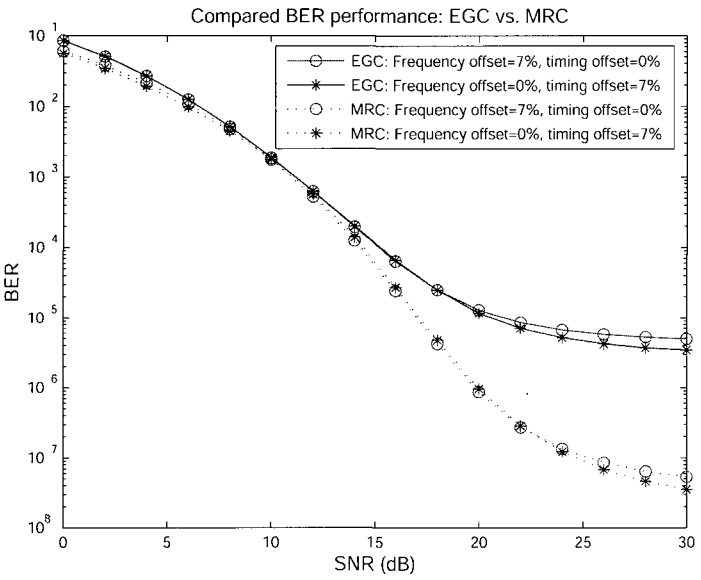

Fig. 5. BER performance comparison: MRC vs EGC, with 64 subcarriers and 10 users.

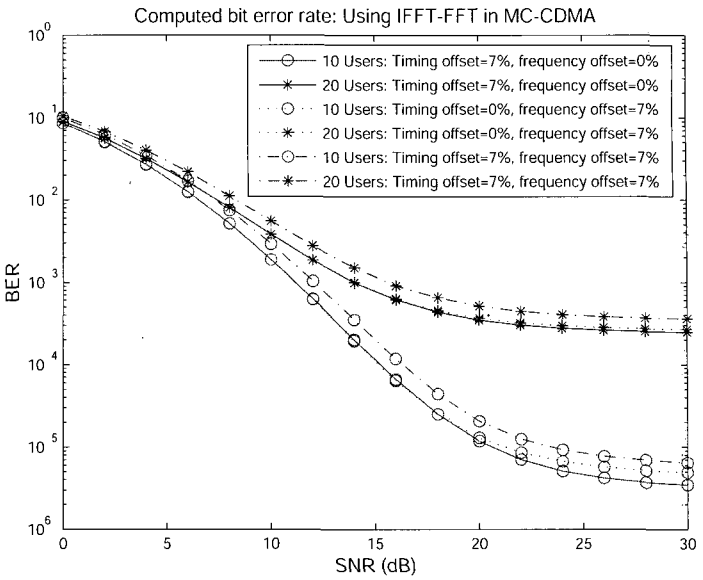

Fig. 6. BER performance comparison between different users. (EGC)

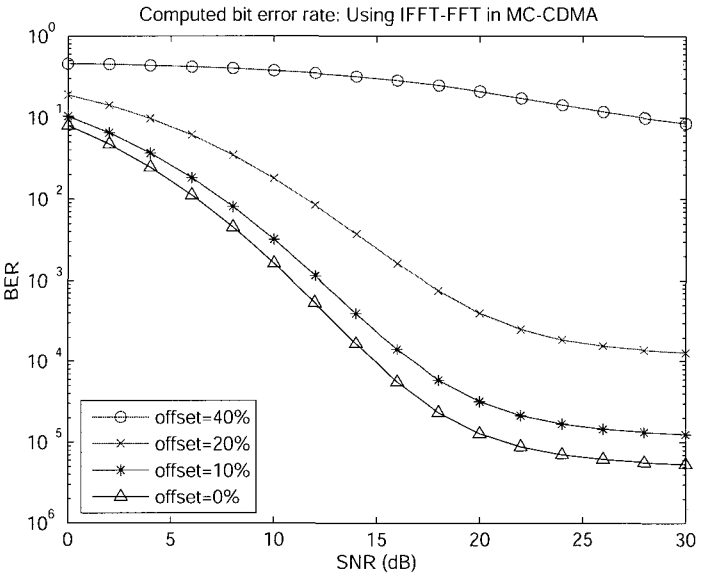

Fig. 7. BERs of an MC-CDMA with 64 subcarriers and 10 users experiencing carrier frequency offsets 0%, 10%, 20%, 40%, respectively, and timing offset 4% . (EGC)

offset will cause the attenuation of the desired signal and the enhancement of the interference signal. The effect of the timing offset is slightly smaller than the carrier frequency offset, because the timing offset does not destroy the orthogonality between subcarriers and hence does not introduce ICI.

Fig. 5 shows the performance comparison between MRC and EGC for the MC-CDMA system with 64 subcarriers and 10 users experiencing carrier frequency offset and timing offset. It is obvious that MRC performs better than EGC.

Fig. 6 shows the BER curves of MC-CDMA with 64 subcarriers experiencing both carrier frequency offset and timing offset. The number of users is varied between 10 and 20. As the number of user increases, the degradation in performance increases as well, because of the fact that the ICI_2 term and the MAI term in (14) are proportional to the number of users. Therefore, for two systems having the same number of subcarriers and experiencing the same degree of carrier frequency offset, the system having a larger number of users will experience more performance deterioration than the system having a smaller number of users.

In Fig. 7, we show the system performance under big frequency offsets. The timing offset here is fixed at 4%. From the figure, we can see that when the carrier frequency offset reaches 40%, the performance loss is significant, a BER of 10^{-3} is no longer possible. Hence the system cannot allow big frequency offsets. It can also be concluded that the frequency offset must

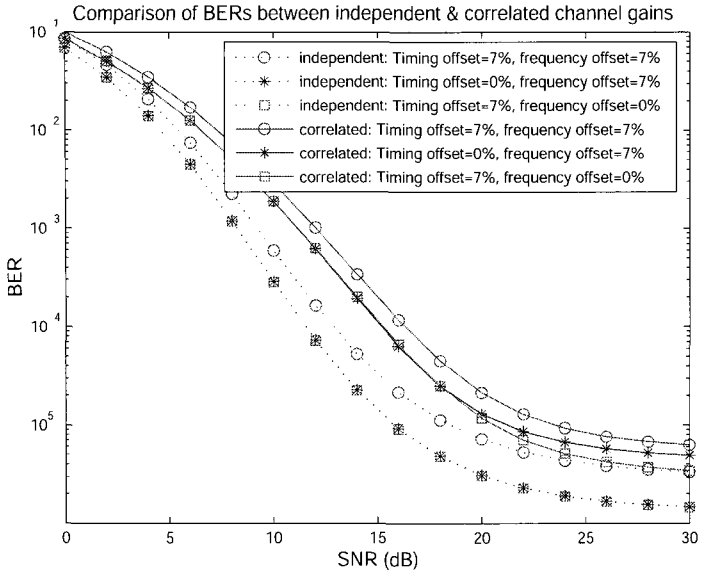

Fig. 8. Comparison of BER performance with different correlation situations. (ECG, 10 users)

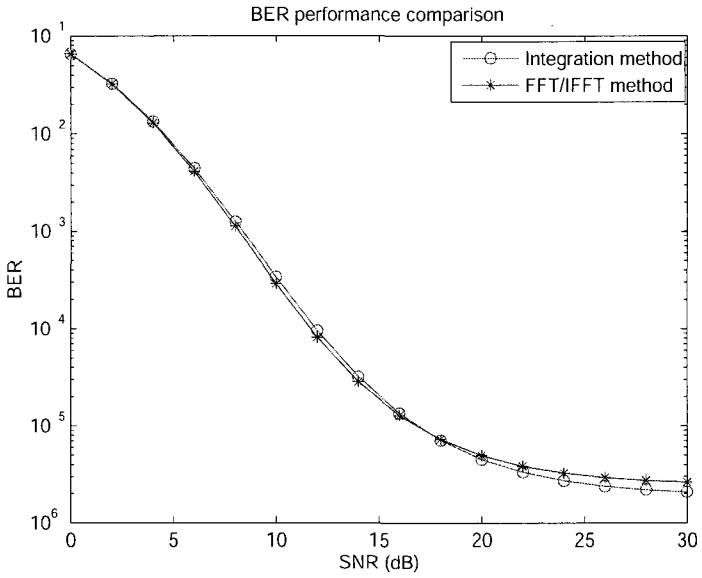

Fig. 9. Comparison of BER performance with conventional MC-CDMA system and proposed MC-CDMA system, with 10% frequency offsets. (EGC)

be kept below 10% to prevent significant performance loss.

In order to observe the effects of correlation between subcarrier channel gains on the BER performance, we plotted the BERs of independent and correlated subcarrier channel gains in Fig. 8. It's easy to see that the system performance is better when the channel gains are mutually independent. We also compare the performance of the MC-CDMA model using IFFT/FFT with that of the conventional model, in order to see which one performs better, and also to verify our numerical analysis. We use [13] as the reference paper, the conventional system model and analysis results are all coming from this paper. Following [13]'s results, we did the simulation under the condition of equal

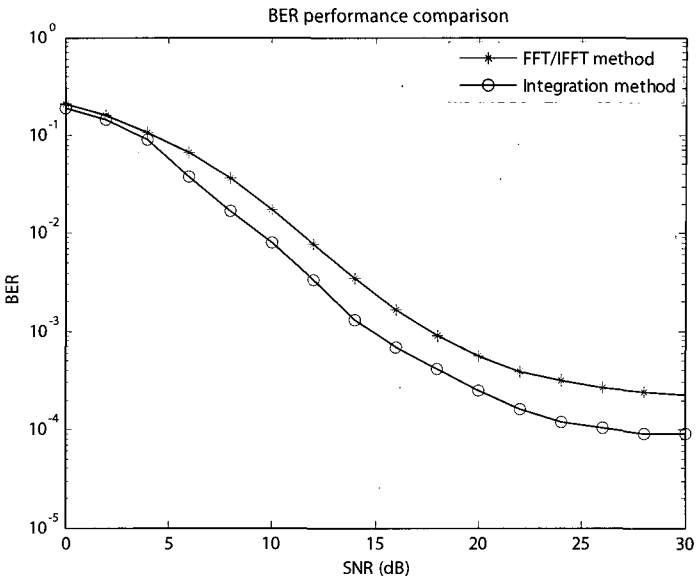

Fig. 10. Comparison of BER performance with conventional MC-CDMA system and proposed MC-CDMA system, with frequency offsets 20%, subcarrier number $N = 16$. (EGC)

gain combining and independent subcarrier channel gain. The subcarrier number is 64 and user number is 10. Fig. 9 shows the performance comparison between the conventional method and the IFFT/FFT method, with 10% frequency offsets, using the exact result. From the simulation result we can see that the performances of the two methods are very close, confirming the equivalence of FFT-based system to conventional system in the presence of frequency offset when N is large, as pointed out in the discussion in Section IV.

Fig. 10 shows the performance comparison between the conventional method and the IFFT/FFT method, with 20% of frequency offset and subcarrier number $N = 16$, using the exact result. From the simulation result we can see that when N is not large enough, the performance of the IFFT/FFT method will suffer more performance degradation than the conventional system. The larger performance degradation suffered by FFT-based system is due to the following facts: In conventional system a correlator is used to demodulate each subcarrier, which observes the received signal over the entire symbol duration. However, FFT-based system only makes use of samples of the received signal for demodulation. While the processing in FFT-based system is simpler, the trade-off is increased performance degradation in the presence of synchronization error.

VI. CONCLUSION

An investigation focusing on the effects of synchronization errors on the BER performance of a downlink MC-CDMA system using FFT/ IFFT has been presented. Analysis has been done for both EGC and MRC. Numerical results indicate that frequency offset, timing offset and channel correlation will cause performance degradation of the MC-CDMA system. A big frequency offset close to or exceeding the frequency spacing between adjacent subcarriers will cause severe BER performance loss. Thus the system cannot allow frequency off-

set that is larger than the frequency spacing between adjacent subcarriers. The comparison between EGC and MRC indicates that MRC performs better. The comparison between the conventional system model shows that when subcarrier number is large, the system using IFFT/FFT has nearly the same performance as the conventional one, while when the subcarrier number is small, the system using IFFT/FFT will suffer worse performance in the presence of carrier frequency offset.

APPENDIX A

After sampling, the signal sample at $t = kT_c + \tau$ is given by

$$r(kT_c+\tau) = \sum_{n=0}^{N-1}\sum_{m=0}^{M-1} d_m c_{n,m}\beta_n e^{j\Phi_n} e^{j2\pi(\frac{n}{NT_c}+\delta f)(kT_c+\tau)} + \eta(kT_c+\tau). \tag{A1}$$

Assuming that user p is the reference user and the frequency offset is less than Δf, the p-th user's i-th chip obtained by FFT can be written as

$$\begin{aligned}\hat{d}_{i,p} =& \frac{1}{N}\sum_{k=0}^{N-1} r(kT_c+\tau)e^{-j2\pi ki/N}\\ =& \frac{1}{N}\sum_{k=0}^{N-1}\sum_{n=0}^{N-1}\sum_{m=0}^{M-1}[d_m c_{n,m}\beta_n e^{j\Phi_n} e^{j2\pi(\frac{n}{NT_c}+\delta f)(kT_c+\tau)}\\ &+\eta(kT_c+\tau)]e^{-j2\pi ki/N}\\ =& \frac{1}{N}e^{j2\pi\delta f\tau}\sum_{n=0}^{N-1}\sum_{m=0}^{M-1} e^{j2\pi\frac{n\tau}{NT_c}} d_m c_{n,m}\beta_n e^{j\Phi_n}\\ &\times\sum_{k=0}^{N-1} e^{j2\pi(n-i)\frac{k}{N}} e^{j2\pi\delta f kT_c} + \eta_i'\\ =& \frac{1}{N}e^{j2\pi\delta f\tau}\sum_{n=0}^{N-1}\sum_{m=0}^{M-1} e^{j2\pi\frac{n\tau}{NT_c}} d_m c_{n,m}\beta_n e^{j\Phi_n}\\ &\times(1+e^{j2\pi\frac{1}{N}(n-i+NT_c\delta f)}+e^{j2\pi\frac{2}{N}(n-i+NT_c\delta f)}+\\ &\cdots+e^{j2\pi\frac{N-1}{N}(n-i+NT_c\delta f)})+\eta_i'\end{aligned} \tag{A2}$$

where

$$\eta_i' = \frac{1}{N}\sum_{k=0}^{N-1}\eta(kT_c+\tau)e^{-j2\pi ki/N}. \tag{A3}$$

We observe that $\{1, e^{j2\pi\frac{1}{N}(n-i+NT_c\delta f)}, e^{j2\pi\frac{2}{N}(n-i+NT_c\delta f)}, \cdots, e^{j2\pi\frac{N-1}{N}(n-i+NT_c\delta f)}\}$ is a geometric series for which the ratio of each two consecutive terms is $e^{j2\pi\frac{1}{N}(n-i+NT_c\delta f)}$. Thus, we have

$$\hat{d}_{i,p} = \eta_i' + \frac{e^{j2\pi\delta f\tau}}{N}\sum_{m=0}^{M-1}\sum_{n=0}^{N-1} e^{j2\pi\frac{n\tau}{NT}}\frac{e^{j2\pi(n-i+\frac{\delta f}{\Delta f})}-1}{e^{j2\pi(n-i+\frac{\delta f}{\Delta f})/N}-1} d_m c_{n,m}\beta_n e^{j\Phi_n}. \tag{A4}$$

The p-th user's i-th chip can then be written as

$$\begin{aligned}\hat{d}_{i,p} =& \eta_i' + \frac{1}{N}P\cdot e^{j\frac{2\pi}{N}\cdot\frac{\tau}{T_c}(i+\frac{\delta f}{\Delta f})} d_p c_{i,p}\beta_i e^{j\Phi_i}\\ &+\frac{1}{N}\sum_{\substack{m=0\\ m\neq p}}^{M-1} P\cdot e^{j\frac{2\pi}{N}\cdot\frac{\tau}{T_c}(i+\frac{\delta f}{\Delta f})} d_m c_{i,m}\beta_i e^{j\Phi_i}\\ &+\frac{1}{N}\sum_{m=0}^{M-1}\sum_{\substack{n=0\\ n\neq i}}^{N-1} Q(n,i)\cdot e^{j\frac{2\pi}{N}\cdot\frac{\tau}{T_c}(n+\frac{\delta f}{\Delta f})} d_m c_{n,m}\beta_n e^{j\Phi_n}\end{aligned} \tag{A5}$$

where

$$P = \frac{e^{j2\pi\frac{\delta f}{\Delta f}}-1}{e^{j2\pi\frac{\delta f}{N\cdot\Delta f}}-1}, \quad Q(n,i) = \frac{e^{j2\pi(n-i+\frac{\delta f}{\Delta f})}-1}{e^{j2\pi(n-i+\frac{\delta f}{\Delta f})/N}-1}.$$

APPENDIX B

Using EGC as an example, the despread signal of user p can be written as

$$\begin{aligned}\hat{d}_p =& \sum_{i=0}^{N-1} d_{i,p}'\\ =& \sum_{i=0}^{N-1}\eta_i'\cdot c_{i,p}e^{-j\Phi_i} + \frac{1}{N}P\sum_{i=0}^{N-1} e^{j\frac{2\pi}{N}\cdot\frac{\tau}{T_c}(i+\frac{\delta f}{\Delta f})} d_{i,p}\beta_i\\ &+\frac{1}{N}P\sum_{i=0}^{N-1}\sum_{\substack{m=0\\ m\neq p}}^{M-1} e^{j\frac{2\pi}{N}\cdot\frac{\tau}{T_c}(i+\frac{\delta f}{\Delta f})} d_{i,m}c_{i,m}c_{i,p}\beta_i\\ &+\sum_{i=0}^{N-1}\sum_{m=0}^{M-1}\sum_{\substack{n=0\\ n\neq i}}^{N-1}\frac{Q(n,i)}{N} e^{j\frac{2\pi}{N}\frac{\tau}{T_c}(i+\frac{\delta f}{\Delta f})} d_{n,m}c_{n,m}c_{i,p}\beta_n\\ &\times e^{j(\Phi_n-\Phi_i)}.\end{aligned} \tag{B1}$$

As defined in Section IV, $P = \frac{e^{j2\pi\frac{\delta f}{\Delta f}}-1}{e^{j2\pi\frac{\delta f}{N\cdot\Delta f}}-1}$. Defining $\alpha = 2\pi\frac{\delta f}{\Delta f}$, $\beta = 2\pi\frac{\delta f}{N\cdot\Delta f}$, then the first term of the right hand side (RHS) of (B1) can be written as $\frac{1}{N}\frac{e^{j\alpha}-1}{e^{j\beta}-1}\sum_{i=0}^{I-1} d_{i,p}\beta_i$. Thus finding the real part of this term is equivalent to determining the real part of P/N

$$\begin{aligned}&\mathrm{Re}[\frac{1}{N}\frac{e^{j\alpha}-1}{e^{j\beta}-1}]\\ &= \frac{1}{N}\mathrm{Re}[\frac{(\cos\alpha-1)+j\sin\alpha}{(\cos\beta-1)+j\sin\beta}]\\ &= \frac{1}{N}\cdot\frac{[(\cos\alpha-1)(\cos\beta-1)+\sin\alpha\sin\beta]}{2(1-\cos\beta)}\\ &= \frac{1}{N}\cdot\frac{\cos(\alpha-\beta)-\cos\alpha-\cos\beta+1}{2(1-\cos\beta)}\\ &= \frac{1}{N}\cdot\frac{2\cos^2\frac{(\alpha-\beta)}{2}-2\cos\frac{(\alpha+\beta)}{2}\cos\frac{(\alpha-\beta)}{2}}{2\cdot 2\sin^2\frac{\beta}{2}}\\ &= \frac{1}{N}\cdot\frac{\cos\frac{(\alpha-\beta)}{2}\cdot\sin\frac{\alpha}{2}}{\sin\frac{\beta}{2}}.\end{aligned} \tag{B2}$$

Similarly, we can obtain the real part of the second term of the RHS of (B1) by substituting $2\pi(n-i+\frac{\delta f}{\Delta f}), 2\pi(n-i+\frac{\delta f}{\Delta f})/N, \Phi_n-\Phi_i+\frac{2\pi}{N}\cdot\frac{\tau}{T_c}(i+\frac{\delta f}{\Delta f})$ with α,β,γ, respectively.

$$\begin{aligned}
&\mathrm{Re}[\frac{1}{N}e^{j\gamma}\frac{e^{j\alpha}-1}{e^{j\beta}-1}]\\
&=\frac{1}{N}\mathrm{Re}[(\cos\gamma+j\sin\gamma)\frac{(\cos\alpha-1)+j\sin\alpha}{(\cos\beta-1)+j\sin\beta}]\\
&=\frac{1}{N}\cdot\frac{\cos(\alpha-\beta+\gamma)-\cos(\alpha+\gamma)-\cos(\gamma-\beta)+\cos\gamma}{2(1-\cos\beta)}\\
&=\frac{1}{N}\cdot\frac{\cos(\gamma+\frac{\alpha-\beta}{2})(\cos\frac{\alpha-\beta}{2}-\cos\frac{\alpha+\beta}{2})}{2\sin^2\frac{\beta}{2}}\\
&=\frac{1}{N}\cdot\frac{\cos(\gamma+\frac{\alpha-\beta}{2})\sin\frac{\alpha}{2}}{\sin\frac{\beta}{2}}.
\end{aligned}\tag{B3}$$

Thus, the real part of (B1) is given by

$$\begin{aligned}
\mathrm{Re}(\hat{d}_p)=&\sum_{i=0}^{N-1}P'\cdot d_{i,p}\beta_i+\mathrm{Re}(\sum_{i=0}^{N-1}\eta_i'\cdot c_{i,p}e^{-j\Phi_i})\\
&+\sum_{i=0}^{N-1}\sum_{m=0}^{M-1}\sum_{\substack{n=0\\n\neq i}}^{N-1}Q'(n,i)\cdot d_m c_{n,m}c_{i,p}\beta_n
\end{aligned}\tag{B4}$$

where

$$P'=\frac{\cos[(1-\frac{1}{N})\cdot\pi\cdot\frac{\delta f}{\Delta f}+\frac{2\pi}{N}\cdot\frac{\tau}{T_c}(i+\frac{\delta f}{\Delta f})]\sin(\pi\frac{\delta f}{\Delta f})}{N\cdot\sin(\pi\frac{\delta f}{N\cdot\Delta f})}.\tag{B5}$$

$$\begin{aligned}
Q'(n,i)=&\sin[\pi(n-i+\frac{\delta f}{\Delta f})]\\
\times&\frac{\cos[\pi(n-i+\frac{\delta f}{\Delta f})(1-\frac{1}{N})+\frac{2\pi}{N}\frac{\tau}{T_c}(i+\frac{\delta f}{\Delta f})+(\Phi_n-\Phi_i)]}{N\sin[\pi(n-i+\frac{\delta f}{\Delta f})/N]}.
\end{aligned}\tag{B6}$$

APPENDIX C

The mean and the variance of the decision variable U_p given by (15) are derived in this Appendix. Two cases are considered in the following.

Case 1: $\{h_n, n=0,1,\cdots,N-1\}$ *are Mutually Independent*

We assume that β_n, Φ_n are independent random variables, it is easy to show that all terms in the summations of (16)–(19) are independent, and these summations are mutually independent. According to the central limit theorem, we employ the Gaussian approximation, known to provide good results for large number of users and long codes. It is readily shown that ICI_1, ICI_2, and MAI are approximately Gaussian with zero mean, hence we only need to determine their variances.

Assuming a "one" is transmitted, the mean and variance of the desired signal D_p are given by

$$E(D_p)=E(\sum_{i=0}^{N-1}P'\cdot d_{i,p}\beta_i)=P'\cdot\sum_{i=0}^{N-1}E(\beta_i)\tag{C1}$$

$$Var(D_p)=Var(\sum_{i=0}^{N-1}P'\cdot d_{i,p}\beta_i)=P'^2\cdot\sum_{i=0}^{N-1}Var(\beta_i).\tag{C2}$$

The variance of ICI_1 is

$$\begin{aligned}
&Var[\sum_{i=0}^{N-1}\sum_{\substack{n=0\\n\neq i}}^{N-1}Q'(n,i)\cdot d_{n,p}c_{n,p}c_{i,p}\beta_n]\\
&=\sum_{i=0}^{N-1}\sum_{\substack{n=0\\n\neq i}}^{N-1}Var[Q'(n,i)\cdot d_{n,p}c_{n,p}c_{i,p}\beta_n]\\
&=\sum_{i=0}^{N-1}\sum_{\substack{n=0\\n\neq i}}^{N-1}Var[Q'(n,i)\beta_n].
\end{aligned}\tag{C3}$$

Similarly, the variance of ICI_2 is

$$\begin{aligned}
&Var[\sum_{i=0}^{N-1}\sum_{\substack{m=0\\m\neq p}}^{M-1}\sum_{\substack{n=0\\n\neq i}}^{N-1}Q'(n,i)\cdot d_{n,m}c_{n,m}c_{i,p}\beta_n]\\
&=\sum_{i=0}^{N-1}\sum_{\substack{m=0\\m\neq p}}^{M-1}\sum_{\substack{n=0\\n\neq i}}^{N-1}Var[Q'(n,i)\cdot d_{n,m}c_{n,m}c_{i,p}\beta_n]\\
&=(M-1)\cdot\sum_{i=0}^{N-1}\sum_{\substack{n=0,\\n\neq i}}^{N-1}Var[Q'(n,i)\beta_n].
\end{aligned}\tag{C4}$$

The variance of MAI is

$$\begin{aligned}
&Var[\sum_{i=0}^{N-1}\sum_{\substack{m=0\\m\neq p}}^{M-1}P'\cdot d_{i,m}c_{i,m}c_{i,p}\beta_i]\\
&=(M-1)\cdot P'^2\cdot Var[\sum_{m\neq p}d_{n,m}\sum_{i=0}^{N-1}c_{i,m}c_{i,p}\beta_i]\\
&=(M-1)\cdot P'^2\cdot\sum_{i=0}^{N-1}Var[\beta_i].
\end{aligned}\tag{C5}$$

Case 2: $\{h_n, n=0,1,\cdots,N-1\}$ *are Mutually Correlated*

It is easy to see that the interference terms ICI_1, ICI_2, MAI of U_p are zero-mean conditional Gaussian conditioned on $\{\beta_n\}$ and $\{\Phi_n\}$, hence U_p is conditional Gaussian.

Assuming a "one" is transmitted, the desired signal D_p is a constant conditioned on $\{\beta_n\}$

$$D_p|\{\beta_n\}=P'\cdot\sum_{i=0}^{N-1}\beta_i.\tag{C6}$$

The conditional variance of ICI_1 is given by

$$\begin{aligned} &Var[ICI_1|\{\beta_n\},\{\Phi_n\}] \\ &= Var[\sum_{i=0}^{N-1}\sum_{\substack{n=0\\n\neq i}}^{N-1} Q'(n,i)\cdot d_{n,p}c_{n,p}c_{i,p}\beta_n] \\ &= \sum_{i=0}^{N-1}\sum_{\substack{n=0\\n\neq i}}^{N-1}[Q'(n,i)]^2\cdot\beta_n^2\cdot Var[c_{n,p}c_{i,p}] \\ &= \sum_{i=0}^{N-1}\sum_{\substack{n=0\\n\neq i}}^{N-1}[Q'(n,i)]^2\cdot\beta_n^2. \end{aligned} \tag{C7}$$

Similarly, the conditional variance of ICI_2 can be found as

$$\begin{aligned} &Var[ICI_2|\{\beta_n\},\{\Phi_n\}] \\ &= Var[\sum_{i=0}^{N-1}\sum_{\substack{m=0\\m\neq p}}^{M-1}\sum_{\substack{n=0\\n\neq i}}^{N-1} Q'(n,i)\cdot d_{n,m}c_{n,m}c_{i,p}\beta_n] \\ &= \sum_{i=0}^{N-1}\sum_{\substack{m=0\\m\neq p}}^{M-1}\sum_{\substack{n=0\\n\neq i}}^{N-1}[Q'(n,i)]^2\cdot\beta_n^2 Var[c_{n,m}c_{i,p}] \\ &= (M-1)\cdot\sum_{i=0}^{N-1}\sum_{\substack{n=0,\\n\neq i}}^{N-1}[Q'(n,i)]^2\cdot\beta_n^2. \end{aligned} \tag{C8}$$

The conditional variance of MAI can be written as

$$\begin{aligned} &Var[MAI|\{\beta_n\},\{\Phi_n\}] \\ &= Var[\sum_{i=0}^{N-1}\sum_{\substack{m=0\\m\neq p}}^{M-1} P'\cdot d_{i,m}c_{i,m}c_{i,p}\beta_i] \\ &= (M-1)\cdot P'^2\cdot Var[\sum_{m\neq p} d_{n,m}\sum_{i=0}^{N-1} c_{i,m}c_{i,p}\beta_i^2] \\ &= (M-1)\cdot P'^2\cdot\sum_{i=0}^{N-1}\beta_i^2. \end{aligned} \tag{C9}$$

REFERENCES

[1] S. Hara and R. Prasad, "An overview of multicarrier CDMA," *IEEE Commun. Mag.*, pp. 126–133, Dec. 1997.

[2] A. C. McCormick and E. A. AI-Susa, "Multicarrier CDMA for future generation mobile communication," *IEEE Electron. Commun. Eng. J.*, vol. 14, pp. 52–60, Apr. 2002.

[3] R. V. Nee and R. Prasad, *OFDM for Wireless Multimedia Communications*, Artech House Publishers, 2000.

[4] H. Liu, *Signal Processing Applications in CDMA Communications*, Artech House Publishers, 2000.

[5] S. B. Weinstein and P. M. Ebert, "Data transmission by frequency-division multiplexing using the discrete Fourier transform," *IEEE Trans. Commun. Technol.*, vol. 19, pp. 628–634, Oct. 1971.

[6] J. A. C. Bingham, "Multicarrier modulation for data transmission: An idea whose time has come," *IEEE Commun. Mag.*, pp. 5–14, May 1990.

[7] T. Keller, L. Piazzo, P. Mandarini, and L. Hanzo, "Orthogonal frequency division multiplex synchronization techniques for frequency-selective fading channels," *IEEE J. Select. Areas Commun.*, vol. 19, pp. 999–1008, June 2001.

[8] L. Tomba and W. A. Krzymien, "Sensitivity of the MC-CDMA access scheme to carrier phase noise and frequency offset," *IEEE Trans. Veh. Tech.*, vol. 48, pp. 1657–1665, Sept. 1999.

[9] D. Kivanc and H. Liu, "Uplink performance of MC-CDMA in the presence of frequency offset," in *Proc. IEEE VTC'99*, vol. 5, 1999, pp. 2855–2859.

[10] J. Jang and K. B. Lee, "Effects of frequency offset on MC/CDMA system performance," *IEEE Commun. Lett.*, vol. 3, pp. 196–198, July 1999.

[11] Y. Kim, K. Bang, S. Choi, C. You, and D. Hong "Effect of carrier frequency offset on performance of MCCDMA systems," *IEE Electron. Lett.*, vol. 35, pp. 378–379, Mar. 1999.

[12] Q. Shi and M. Latva-aho, "Effect of frequency offset on the performance of asynchronous MC-CDMA systems in a correlated Rayleigh fading channel," in *Proc. IEEE ICC 2001*, vol. 2, pp. 448–452, 2001.

[13] Y. Kim, S. Choi, C. You, and D. Hong, "BER computation of an MC-CDMA system with carrier frequency offset," in *Proc. IEEE Int. Conf. Acoustics, Speech, Signal Processing*, vol. 5, 1999, pp. 2555–2558.

[14] T. Kim, Y. Kim, J. Park, K. Ko, S. Choi, C. Kang, and D. Hong, "Performance of an MC-CDMA system with frequency offsets in correlated fading," in *Proc. IEEE ICC 2000*, vol. 2, 2000, pp. 1095–1099.

[15] X. Gui and T. S. Ng, "Performance of asynchronous orthogonal multicarrier CDMA system in frequency selective fading channel," *IEEE Trans. Commun.*, vol. 47, pp. 1084–1091, July 1999.

[16] H. Steendam and M. E. Moeneclaey, "The sensitivity of downlink MC-DS-CDMA to carrier frequency offsets,"*IEEE Commun. Lett.*, vol. 5, pp. 215–217, May 2001.

[17] T. S. Rappaport, *Wireless Communications, Principles & Practice*, Prentice Hall PTR, 1996.

[18] T. Eng and L. B. Milstein, "Coherent DS-CDMA performance in Nakagami multipath fading," *IEEE Trans. Commun.*, vol. 43, pp. 1134–1143, Feb./Mar./Apr. 1995.

[19] E. A. Sourour and M. Nakagawa, "Performance of orthogonal multicarrier CDMA in a multipath fading channel," *IEEE Trans. Commun.*, vol. 44, pp. 356–367, Mar. 1996.

[20] W. H. Press, B. P. Flannery, S. A. Teukolsky, and W. T. Vetterling, *Numerical Recipes: The Art of Scientific Computing*, New York: Cambridge Univ. Press, 1986.

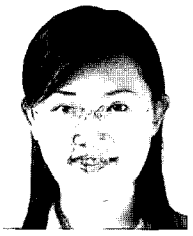

Ying Li received B.E. degree from Beijing University of Posts and Communications, Beijing, China, in 2001 and M.S. degree from National University of Singapore, Singapore, in 2005, both in Electrical Engineering. Currently, she is an engineer at Singapore Motorola Development Center. Her research interests include wireless communications, multicarrier transmissions, and cooperative networks.

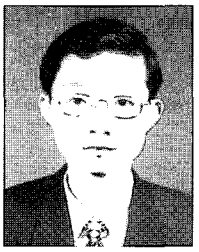

Xiang Gui received B.S. and M.S. degrees from Shanghai Jiao Tong University, China, in 1991 and 1994, respectively, and the Ph.D. degree from the University of Hong Kong in 1998, all in electrical engineering. Currently, he is a lecturer in Communication Engineering at the Institute of Information Sciences and Technology, Massey University, New Zealand. Prior to joining Massey in 2003, he worked at Nanyang Technological University, Singapore, and Shanghai Jiao Tong University, China. His research interests include wireless and mobile communications & applications, multicarrier & spread spectrum systems, and communication networks.